ACS Chemical Neuroscience

Review

pubs.acs.org/chemneuro

Imaging Chemical Neurotransmission with Genetically Encoded Fluorescent Sensors

Ruqiang Liang,[†] Gerard Joseph Broussard,[†,‡] and Lin Tian*[,†,‡]

[†]Department of Biochemistry and Molecular Medicine and [‡]Center for Neuroscience, University of California Davis, Davis, California 95817, United States

ABSTRACT: A major challenge in neuroscience is to decipher the logic of neural circuitry and to link it to learning, memory, and behavior. Synaptic transmission is a critical event underlying information processing within neural circuitry. In the extracellular space, the concentrations and distributions of excitatory, inhibitory, and modulatory neurotransmitters impact signal integration, which in turn shapes and refines the function of neural networks. Thus, the determination of the spatiotemporal relationships between these chemical signals with synaptic resolution in the intact brain is essential to decipher the codes for transferring information across circuitry and systems. Here, we review approaches and probes that have been employed to determine the spatial and temporal extent of neurotransmitter dynamics in the brain. We specifically focus on the design, screening, characterization, and application of genetically encoded indicators directly probing glutamate, the most abundant excitatory neurotransmitter. These indicators provide synaptic resolution of glutamate dynamics with cell-type specificity. We also discuss strategies for developing a suite of genetically encoded probes for a variety of neurotransmitters and neuromodulators.

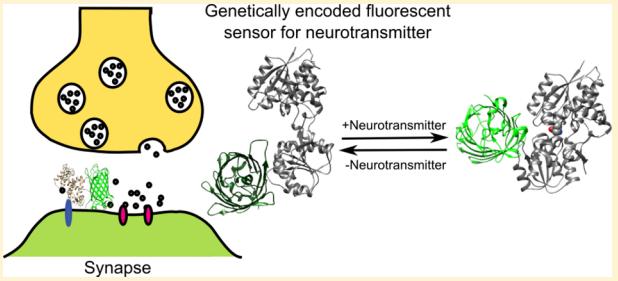

KEYWORDS: *Neurotransmitter, neuromodulator, optical probes, genetically encoded indicators, iGluSnFR, fluorescent sensor, synapse*

The human brain contains billions of neurons interconnected by trillions of synapses to yield the circuitry that is the "wiring" of the brain. Synapses are important structural and functional units for neuronal communication, where axons project from local or distant presynaptic neurons to make contact with dendrites of postsynaptic neurons. Past and recent studies using electrophysiology and imaging have developed a picture of the functional and morphological characteristics of synaptic connections. The arrival of an action potential (AP) at a synapse triggers the fusion of neurotransmitter-containing vesicles followed by release of neurotransmitters (NTs) into a nanometer scale synaptic cleft or in some cases at nonsynaptic sites.[1] Following release, neurotransmitters cross the synapse and bind to the receptors located on postsynaptic neurons. They also activate autoreceptors or receptors at extrasynaptic sites.

At the molecular level, the probability of neurotransmitter release can be highly variable and changes over time.[2] In addition to changes in the amounts of NT release, depolarization of postsynaptic neurons in response to presynaptic AP output depends on the type, expression level, and phosphorylation state of postsynaptic receptors and their association with regulatory proteins. At the cellular level, the number and distribution of excitatory and inhibitory inputs, such as those that utilize glutamate or γ-aminobutyric acid (GABA) to interact with ligand-gated ion channels, onto individual neurons has a significant impact on signal integration, which in turn shapes and refines the function of neural circuitry. In addition, neuromodulators, such as dopamine, typically interacting with postsynaptic G-protein coupled receptors, reconfigure the dynamics of neural circuitry by transforming the intrinsic firing properties of targeted neurons and regulating their synaptic plasticity. Some NTs, such as serotonin and acetylcholine, have dual functions as both neuromodulators and classical NTs. The altered dynamics of neurotransmitters and neuromodulators have been implicated in a number of human neurological and psychiatric diseases, including Parkinson's disease, schizophrenia, and addiction.[3,4]

To date, more than 100 NTs and neuromodulators have been discovered in the brain.[5] Although the anatomical characterization and functional significance of NT-specific projections are understood to a moderate degree, the precise mechanisms by which these molecules regulate the dynamics of healthy and diseased neural circuitry are not fully understood. Gaining an understanding of these mechanisms will involve sensitive, specific, and direct measurements of the type and magnitude of NT transients produced during release events with single-neuron or single-synapse resolution and the requisite temporal resolution in cell culture, tissue preparations, and intact circuits.

Special Issue: Monitoring Molecules in Neuroscience 2014

Received: November 4, 2014
Revised: January 6, 2015
Published: January 7, 2015

 © 2015 American Chemical Society

DOI: 10.1021/cn500280k
ACS Chem. Neurosci. 2015, 6, 84−93

CURRENT APPROACHES FOR DIRECT MEASUREMENT OF CHEMICAL TRANSMISSION IN THE BRAIN

Existing methods, including fast-scan cyclic voltammetry (FSCV)[6] and microdialysis[7] have been broadly used for direct measurement of NT release and uptake in cell culture, brain slices, and awake animals engaged in a variety of behavioral tasks. FSCV combined with carbon-fiber microelectrodes can detect electrochemically active NTs, most notably dopamine (DA), in the nanomolar range on the time scale of milliseconds. Application of FSCV has provided a deep understanding of the functional roles of DA dynamics in shaping neural circuitry both ex vivo and in vivo, in the latter case in anesthetized and behaving animals.[6,8] Modified (sawhorse) FSCV waveforms have been introduced that push the detection limits of DA down to ~1 nM in vitro.[9] However, FSCV detection of DA and other biogenic amines, such as norepinephrine, epinephrine, and serotonin, can be convoluted due to the lack of specificity of electrochemical detection (i.e., multiple species are oxidized or reduced at overlapping potentials). Further, despite superior temporal resolution compared to microdialysis and some imaging approaches, voltammetry alone does not reveal cell-type specificity and has only moderate spatial resolution for the study of signaling events due to the probe size. It is impossible to isolate single axons when recording with microelectrodes within the neuropil and to identify single synapses or release sites.

Electrochemically inactive NTs, such as glutamate, GABA, and glycine, are measured in situ using microdialysis coupled with high performance liquid chromatography, capillary electrophoresis, mass spectroscopy, and nanotechnology-based approaches.[7] The spatial and temporal resolution of microdialysis has been greatly improved via advances in probe fabrication and the sensitivity of detection methods. For example, microlithography manufacturing of smaller microdialysis probes permits sampling volumes as small as 4 nL. Segmentation of dialysates into nanoliter droplets through the use of a microfluidic tee mounted directly on the heads of test subjects enables temporal sampling resolution on the scale of a few seconds.[7] Despite these advances and superior chemical selectivity, microdialysis is far from enabling single synapse resolution.[10]

Enzyme-based electrochemical biosensors have also been used for indirect measurement of nonelectrochemically active NTs, such as glutamate and acetylcholine, as well as other chemical signaling molecules and glucose use in the brain. However, this approach also lacks cellular resolution, can potentially lose sensitivity in biological tissues, and can be cofounded by other potential sources of naturally occurring electroactive molecules.[11,12]

POSITRON EMISSION TOMOGRAPHY (PET) AND FUNCTIONAL MAGNETIC RESONANCE IMAGING (fMRI)

Macroscale imaging modalities, such as positron emission tomography (PET) and functional magnetic resonance imaging (fMRI), are used to measure physiological function primarily in humans but also in experimental animals. These noninvasive methods provide information on the connectivity and dynamics of neural activity over large brain volumes. PET combined with radiolabeled metabolites or receptor agonists or antagonists has been extensively used as a surrogate to study the dynamics of chemical neurotransmission at the circuitry level.[13] However, the spatial resolution of PET is a few millimeters and temporal resolution is a few minutes.[14] fMRI depends on radiofrequency electromagnetic energy that readily penetrates the skull to image brain function without exposure to ionizing radiation. Clinically, fMRI has replaced many functions of PET in diagnostic imaging to identify brain areas involved in specific motor and cognitive tasks. Most recently, with the development of NT-sensitive contrast agents, fMRI was used for the first time for mapping the dynamics of NT release and signaling in deep brain regions with molecular specificity and requisite spatial coverage.[15]

Paramagnetic metalloproteins are MRI contrast agents that are amenable to protein engineering strategies for the development of ligand-sensitive MRI probes for molecular imaging. The bacterial cytochrome P450-BM3 heme domain (BM3h) is an attractive scaffold for MRI sensor design, as this protein can be modified to improve stability and alter substrate specificity via directed evolution and rational design approaches.[16] Recently, a family of NT-sensitive MRI contrast agents based on BM3h has thus been developed. A BM3h sensor variant, called BM3h-9D7, displaying specificity for dopamine (K_d = 1.3 μM for DA; 37 and 70 μM for norepinephrine and serotonin, respectively), has been used for quantitatively mapping dopamine release in the ventral striatum (a brain region involved in processing rewards) in living rat brains.[15,17] Specifically, BM3h-9D7 was injected intracranially to fill the entire ventral striatum that is several cubic millimeters. Following electrical stimulation of the medial forebrain bundle in the lateral hypothalamus, MRI was repeatedly performed to yield time-resolved volumetric measurement of DA release. This work laid the foundation for the development and application of molecular fMRI techniques in neural circuitry mapping with a spatial resolution below 100 μm, and a temporal resolution of seconds, which is an order of magnitude better than PET.[14] Despite the advancement of fMRI probes and human compatibility, spatial and temporal resolution in optimized in vivo preparations for fMRI still lag behind the threshold required to image signaling events at single synapses by at least 2 orders of magnitude.

DIRECT OPTICAL MEASUREMENT OF NTs WITH FLUORESCENCE MICROSCOPY

Fluorescent microscopy combined with optical sensors, on the other hand, is highly appealing to neuroscientists, as it can potentially reach the spatiotemporal resolution required for measuring activity at individual synapses (~1 μm and ms to s time scale) in cultured cells, brain tissue, and intact brains. Fluorescence microscopy systems based on one-photon (1P) or multiphoton have been developed and optimized to enhance imaging depth, to increase imaging speed, and to improve spatial resolution. For example, imaging depths of ~1600 μm have been achieved with two-photon imaging while maintaining excellent spatial resolution in intact mammalian preparations for structural imaging.[18] For functional imaging of calcium transients with a genetically encoded calcium indicator (GCaMP6s), three-photon microscopy at 1300 nm excitation has been used to image layer 6 of adult mouse cortex, at about a 700 μm depth (personal communication with Xu et al., and refs 19 and 20). Several miniaturized 1P fluorescence microscopes have been developed that enable imaging of calcium transients with either organic dye[21] or GCaMPs[22] at arbitrary brain depths in freely moving mice and rats. Super-high-resolution

DOI: 10.1021/cn500280k
ACS Chem. Neurosci. 2015, 6, 84−93

Table 1. Performance of Existing Fluorescent Sensors for Neurotransmitters on Cell Surfaces

name	scaffold	K_d (glutamate)	K_d (aspartate)	K_d (glutamine)	max ΔR or $\Delta F/F$	K_{off} (s^{-1})	neuronal culture	in vivo
EOS[40]	iGluR2(S1S2)	148 nM	n.d.	n.d.	0.21	0.67	yes	no
K716A-EOS[41]	S1S2-K716A	174 nM	n.d.	n.d.	0.29	0.35	yes	no
L401C-EOS[41]	S1S2-L401C	1.57 μM	n.d.	n.d.	0.48	3.7	yes	yes
Snifit-iGluR5[45]	iGluR5(S1S2)	15 μM	n.d.	n.d.	1.56, 1.93[b]	n.d.	no	no
GABA-Snifit[44]	$GABA_B$	100 μM[a]	n.d.	n.d.	1.8	0.35	no	no
GABA-Snifit-GB1/2[44]	GB1/2	420 μM[a]	n.d.	n.d.	1.4	n.d.	no	no
FLIPE-600n[59]	GltI-WT	600 nM[b]	6 μM	100 μM	0.27[b]	n.d.	yes	no
FLIPE-10μ[59]	GltI-A207R	10 μM[b]	60 μM[b]	1 mM[b]	0.15[c]	n.d.	yes	no
FLII[81]E-1μ[61]	GltI-N81V-ECFP-Q82N	1 μM[b]	n.d.	n.d.	0.48[b]	n.d.	yes[f]	no
GluSnFN[62]	GltI-WT	150 nM[b]	700 nM[b]	30 μM[b]	0.18[b]	15	no	no
superGluSnFR[63]	GltI-S73T	2.5 μM[b]	n.d.	n.d.	0.44[b]	75	yes	no
iGluSnFR[65]	GltI-A207V	107 μM,[b] 4.9 μM[c]	145 μM[b]	n.d.	4.5[b], 1.03[c]	n.d.[e]	yes	yes

[a]Not for glutamate but for GABA. [b]Titration with purified protein in solution. [c]In situ affinity of the sensor on the neuron surface. [d]Reported peak time 63 ms and half-width of 238 ms in response to evoked glutamate release in cortical brain slices. [e]K_{on} was above the detection limit of the stop-flow instrument. Instead, $t_{1/2}$ was measured in iGluSnFR-expressing neuron in response to field potential stimulation. $t_{1/2}$ on is 15 ms, and $t_{1/2}$ off is 92 ms. [f]Not in dissociated neuronal culture but in brain slices.

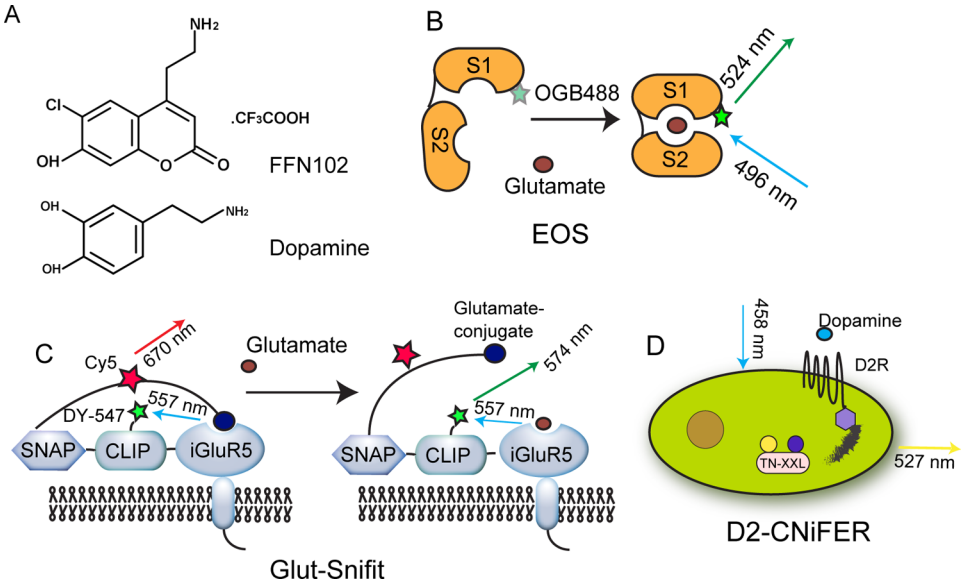

Figure 1. Synthetic and semigenetically encoded fluorescent sensors for neurotransmitters. (A) Fluorescent false neurotransmitter FFN102 and the neurotransmitter dopamine. FFN102 acts as a substrate for vesicular monoamine transporter 1 and 2 that can load dopamine (DA) and serotonin (5-HT) into synaptic vesicles. It increases fluorescence upon vesicular exocytosis, thus acting as an indirect measurement of the DA or 5-HT release. (B) Glutamate optical sensor (EOS) based on the ligand-binding domain of AMPA receptor GluR2's S1S2 domain. Synthetic fluorescent probe Oregon Green 488 (OG488) is conjugated to the S1S2 domain near the glutamate-binding pocket. Binding of glutamate leads to the increased fluorescence intensity of OG488. (C) Glutamate-Snifit based on ionotropic glutamate receptor iGluR5. Binding of glutamate displaces glutamate antagonist attached to SNAP-tag, which decouples the Föster resonance energy transfer (FRET) between the green donor and red acceptor. (D) Cell-based neurotransmitter fluorescent-engineered reporter (CNiFER) for dopamine, in which HEK293 cells expresses D2 dopaminergic receptor, a G-protein coupled receptor (GPCR) for dopamine. Binding of dopamine to the GPCR on the cell surface leads to intracellular calcium increase that can be detected by a FRET-based genetically encoded calcium indicator (TN-XXL).

microscopy improves spatial resolution beyond the diffraction limit (200−300 nm laterally and 550−700 nm axially) down to the nanometer scale.[23,24] Light-sheet fluorescence microscopy illuminates a thin slice of the sample (nm to μm in depth) and permits imaging a whole larval zebrafish brain with cellular resolution thrice a second.[25] Most recently, lattice light-sheet microscopy has been developed and holds great promise for in vivo three-dimensional (3D) imaging of fast dynamic processes in cells. This optical instrument improves imaging speed by 1−2 orders of magnitude and increases spatial resolution by 2-fold along the *z*-axis over conventional confocal fluorescent microscopy with reduced photobleaching and phototoxicity.[26] It can capture images at speeds of 100−2000 planes per second, allowing 3D image acquisition at subsecond resolution.

As imaging technologies such as these become more developed and available for routine laboratory applications, high-quality optical probes have also been developed to track neural activity. Recent advances in the creation and optimization of small-molecule based and genetically encoded sensors have led to several high-quality optical probes reporting changes in calcium concentration,[27−29] synaptic vesicular fusion,[30−32] and membrane voltage.[33−35] To date, genetically encoded calcium sensors are the most broadly utilized imaging probes for large-scale sensing of neural activity in genetically

DOI: 10.1021/cn500280k
ACS Chem. Neurosci. 2015, 6, 84−93

defined populations in behaving animals. However, the relationship between presynaptic calcium and NT release is nonlinear. NT release is a final result of complex processes involving multiple mechanisms and targets, such as the amount of calcium that enters presynaptic terminals via calcium channels, the number of vesicles available for release as a result of vesicle trafficking and replenishment, the properties and distribution of the synaptic proteins that form the release machinery, and feedback form postsynaptic sites.[2,36,37] Though synaptic release probability can be estimated by imaging and quantifying vesicle exocytosis using sensors reporting synaptic activity, such as synaptopHluorin, or measuring postsynaptic calcium accumulation, both of these approaches lack the ability to report the extent of the spatial spread of NT release. Therefore, sensors that directly measure NTs with molecular specificity are an ultimate objective for applications in which transmitter release and diffusion is the primary concern.

For this, an array of NT probes, ranging from small molecules, small molecule−protein hybrids, cell-based sensors, and protein-based approaches, have been developed to be compatible with fluorescent microscopy. Here, we summarize the design and performance of the state-of-the-art NT sensors in each of these classes (Table 1). We further discuss the strengths and weaknesses of each in fluorescent imaging of NT dynamics.

SMALL-MOLECULE BASED SENSORS FOR NTs

Fluorescent false neurotransmitters (FFNs) are a family of synthetic NT tracers that specifically label synaptic vesicles to enable optical measurement of NT release kinetics at individual synapses. Focusing on the dopaminergic system, the first FFN, FFN511, was developed as a fluorescent substrate for vesicular monoamine transporter 2 (VMAT2).[38] When transported into synaptic vesicles by VMAT2 and released upon exocytosis, the rate of release of FFN511 with respect to a high number of APs (over 100) can be determined by measuring decreased fluorescent intensity representing the remaining FFN at presynaptic sites. To reflect physiologically relevant firing patterns of dopaminergic neurons more accurately, an improved version, FFN102 (Figure 1A), was designed as a pH-sensitive probe. FFN102 shows increased fluorescence upon release triggered by short pulses of APs. These FFNs have been used mostly in mouse brain striatal slices and to enable optical detection of the release dynamics of synaptic content.[39] However, small-molecule based sensors need to be delivered to the release sites of interest and do not reveal cell-type specificity.

SEMIGENETICALLY ENCODED SENSORS FOR NTs

As demonstrated in the case of FFNs, small-molecule fluorophores are effective tools to measure cellular signaling pathways, despite their poor cellular specificity. To put these synthetic dyes under genetic control, a variety of fluorogenic sensors for direct measurement of extracellular NTs based on a protein-fluorophore hybrid design have been developed.

For example, a glutamate optical sensor (EOS, Figure 1B), which is a hybrid sensor constructed from the S1S2 glutamate-binding domain of the AMPA receptor GluR2 subunit and a small-molecule dye (Oregon Green 488 (OG488)), has been engineered and applied to the measurement of glutamate release in mouse acute slices and mouse cortex in vivo. Mutant S403C facilitated labeling of S1S2 with OG488 near the glutamate binding pocket. Upon glutamate binding, EOS undergoes a conformation change that causes the changes in fluorescence emission of OG488 (Figure 1B). The resulting sensor exhibited an increase of 21% in $\Delta F/F_{max}$ (maximal fluorescence changes over basal fluorescence) upon glutamate binding (K_d = 148 nM) when measured at the surface of HeLa cells.[40] The variant K716A-EOS showed a K_d of 174 nM for glutamate and $\Delta F/F_{max}$ of 29%. For the variant L401C-EOS, these values were 1.57 μM and 48%, respectively.[41,42] L401C-EOS showed about a 1−2% fluorescence increase in mouse somatosensory cortical neurons following limb movement.[41]

More recently, Snifit (SNAP-tag based indicator proteins with a fluorescent intramolecular tether)-based sensors for optical measurement of glutamate and GABA have also been developed.[43−45] A Snifit (Figure 1C) is a fusion protein with three components: a natural receptor for a specific analyte, a CLIP-tag with a synthetic donor fluorophore, and a SNAP-tag bearing another synthetic acceptor fluorophore conjugated with an antagonist. In the absence of analyte, the Snifit adopts a closed conformation and Förster resonance energy transfer (FRET), a form of nonradiative energy transfer between two fluorescent molecules, efficiency increases. In the presence of analyte, the intramolecular antagonist is displaced to shift Snifit toward an open state with a resultant decrease in FRET efficiency.

Snifit provides a general scaffold for the design of fluorescent metabolite sensors on cell surfaces via selection of a natural receptor−antagonist pair. For example, GABA-Snifit reporter is based on the metabotropic $GABA_B$ receptor and its antagonist CGP 51783. GABA-Snifit on the surface of mammalian human embryonic kidney (HEK) 293 cells allowed detection of perfused GABA with a ratiometric change in donor−acceptor ratio of 1.8-fold and an apparent K_d of 100 μM for GABA.[44] Similarly, glutamate-Snifit (Figure 1C) is based on the ionotropic glutamate receptor 5 (iGluR5) and O6-benzylguanine (BG)-polyethylene glycol (PEG) 11-Cy5-glutamate as the antagonist. This Snifit-iGluR5 showed a ΔR_{max} (maximal fluorescence change in donor−acceptor ratio) of 1.93 and an apparent K_d of 15 μM for glutamate in HEK 293T cells.[45] Further optimization and characterization are likely needed to allow in situ detection of physiological levels of glutamate and GABA release and uptake by living neurons and intact circuitry.

CELL-BASED SENSOR CNiFERs

Recently, cell-based NT fluorescent-engineered reporters (CNiFERs) have been developed to detect NT volume transmission with nM sensitivity.[46,47] CNiFERs consist of HEK 293 cells stably expressing a NT-specific G protein-coupled receptor (GPCR) combined with the FRET-based genetically encoded calcium indicator (TN-XXL) as the readout (Figure 1D). The presence of the GPCR ligand activates an endogenous or chimeric G-protein pathway (Gq proteins activated by Gi/o specific GPCRs) that results in calcium release from internal stores. Activating this pathway in turn increases the FRET efficiency of the TN-XXL.

The first CNiFER, M1-CNiFER, was developed to measure acetylcholine (ACh) dynamics in the extracellular space. M1-CNiFER uses the M1 receptor, a muscarinic G-protein-coupled receptor, to probe ACh concentrations.[46] Additional CNiFERs have been developed to probe in vivo dopamine (D2-CNiFER using D2 dopaminergic receptors) and noradrenaline (α_{1A}-CNiFER using α_{1A} adrenergic receptors) dynamics with nanomolar sensitivity in mouse frontal cortex with temporal

DOI: 10.1021/cn500280k
ACS Chem. Neurosci. 2015, 6, 84−93

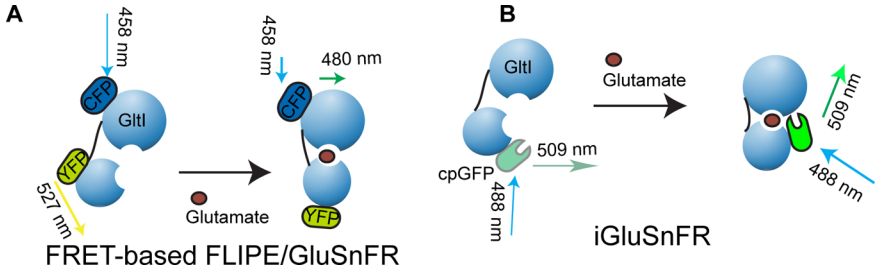

Figure 2. Genetically encoded fluorescent sensors for glutamate. (A) Föster resonance energy transfer (FRET)-based glutamate sensor FLIPE or GluSnFR. Both use periplasmic glutamate-binding protein GltI from *E. coli* as a scaffold. GltI has two lobes joined by a hinge. When there is no glutamate, GltI adopts an open conformation. Binding of glutamate brings GltI to a closed conformation. This conformational change leads to decreased FRET between the N-terminal tagged cyan fluorescent protein and C-terminal tagged yellow fluorescent protein. (B) Circularly permutated green fluorescent protein (cpGFP)-based iGluSnFR. iGluSnFR also uses GltI as glutamate sensing scaffold. Conformational change upon glutamate binding leads to the deprotonation of the fluorophore in cpGFP, thus increasing its fluorescence intensity.

resolution of seconds and spatial resolution of less than 100 μm.[47] This elegant work holds great promise for providing a general platform to engineer cell-based sensors for many different NTs. It may be possible to create CNiFERs using other Gi/o-coupled receptors, such as those for somatostatin, serotonin, and opioid peptides, by redirecting Gi/o-coupled receptors for these ligands to the Gq-calcium signaling pathway.

One limitation is that these cell-based sensors are designed to detect volume transmission of NTs and cannot achieve the resolution required to detect finer patterning in extrasynaptic or synaptic release. Moreover, as the fluorescent signals associated with CNiFERs do not reflect NT levels directly but instead detect downstream changes in intracellular calcium concentrations, their temporal resolution is also limited by the speed of the activation of the G_q pathway used for NT detection. Finally, these probes are composed of cells that must be exogenously introduced to recording sites making them more invasive than some genetically encoded probes (see below).

DESIGN OF GENETICALLY ENCODED FLUORESCENT SENSORS FOR GLUTAMATE

Sensors that are fully protein based (i.e., genetically encodable) can be targeted to specific synapses or genetically defined subpopulations of cells to allow direct, noninvasive, ultrasensitive, and chronic optical measurement of NT dynamics in vitro in cells, ex vivo in tissue, and in vivo in behaving animals. Genetically encoded sensors typically consist of analyte-binding and reporter elements that are based on either a single fluorescent protein (FP) or two FPs. In the case of single FP-based sensors, changes in NT concentrations in the extracellular environment detected by the analyte-binding domain result in changes in the chromophore environment of the FP, such as circularly permutated GFP (cpGFP),[48] leading to an increase or decrease in fluorescence intensity.[49−51] In the case of two FP-based sensors, the conformational changes in the analyte-binding or sensing domain lead to FRET between two FPs that are in close proximity with overlapping excitation and emission spectra.[52,53] FRET-based and single-FP based sensors have different strengths and limitations in the context of specific applications (for review, see refs 54 and 55).

To date, protein-engineering efforts have focused on the development of of glutamate sensors, which have already achieved the requisite spatiotemporal precision to probe neurotransmission at single-cell or single-synapse levels. These sensors consist of the bacterial glutamate/aspartate-binding protein, GltI (also called YbeJ), which functions as the glutamate-binding domain, and a single FP or two FPs as reporter elements. A summary of the performance of these existing glutamate sensors, including FLIPE, GluSnFR, super-GluSnFR, and the recently developed iGluSnFR, are presented in Table 1.

The bacterial protein GltI belongs to a large superfamily of periplasmic binding proteins (PBPs) that are bacterial receptors for a variety of ligands, including carbohydrates, amino acids, dipeptides, and oligopeptides.[56,57] The *Escherichia coli* (*E. coli*) GltI,[58] similar to other PBP family members, undergoes a remarkable, ligand-dependent conformational change, thus providing an ideal scaffold for sensor engineering. It consists of a Venus flytrap module where a hinged region connects two flap domains that bind to ligands at the interface between them. The flap domains can adopt two different conformations: a ligand-free open form and a ligand-bound closed form, which interconvert through a relatively large bending motion around the hinge. The conformational changes of GltI upon glutamate binding can lead to FRET between two properly inserted FPs or to changes in fluorescence of a single FP as readouts for glutamate dynamics.

FRET-BASED GLUTAMATE INDICATORS

The first genetically encoded glutamate indicator, FLIPE, was developed by linearly inserting GltI between an N-terminal enhanced cyan fluorescent protein (ECFP) and a C-terminal yellow fluorescent protein called Venus (Figure 2A).[59] A series of FLIPE sensors with a broad range of affinities (600 nM, 10 μM, 100 μM, and 1 mM) has been engineered to monitor a wide range of glutamate concentrations (100 nM to 100 μM) at the surface of living cells with a reversible concentration-dependent decrease in FRET efficiency. For example, when FLIPE-600n was expressed on the surface of dissociated neurons, the sensor responded to extracellular glutamate (about 300 nM) triggered by electrical depolarization. Further optimization of the ECFP insertion site in GltI (between Asn81 and Gln82) by rational design to restrict the rotational freedom of the chromophores resulted in a highly sensitive glutamate indicator, FLII^{81}E-1μ, which showed increased signal changes (ΔR_{max} = 48%) with a K_d of 1 μM for glutamate.[60,61]

In parallel, another FRET-based glutamate indicator, GluSnFR,[62] was engineered by inserting GltI between ECFP and a yellow fluorescent protein, Citrine (Figure 2A). The first GluSnFR showed high affinity for glutamate (K_d = 150 nM), which might cause partial saturation at background glutamate levels in neuronal systems. Therefore, the affinity of GluSnFR

DOI: 10.1021/cn500280k
ACS Chem. Neurosci. 2015, 6, 84−93

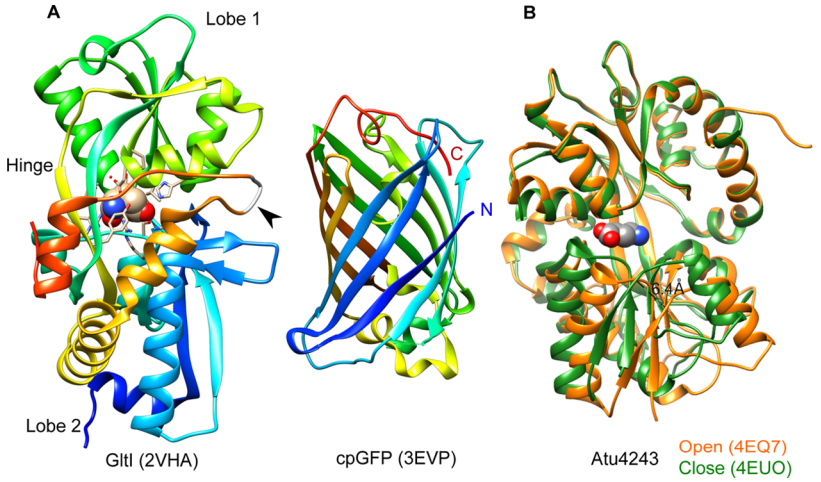

Figure 3. Structures of iGluSnFR and a GABA-binding protein. (A) Crystal structure of GltI (PDB ID: 2VHA) and cpGFP (PDB ID: 3EVP). Both are shown blue to red as N-terminal to C-terminal. Glutamate is shown as spheres. Arrowhead on GltI denotes cpGFP insertion site where cpGFP replaced the sequence shown as gray. Hinge and two lobes of Venus flytrap are labeled. (B) Open (orange, PDB ID: 4EQ7) and close (green, PDB ID: 4EUO) conformation of GABA-binding protein Atu4243 from *Agrobacterium tumefaciens*. GABA is shown as spheres. Black dashed line shows 6.4 Å movement of Gly58 upon GABA binding. Molecular graphics and analyses were performed using UCSF Chimera.

to glutamate was reduced by site-directed mutagenesis of key glutamate binding residues to produce a series of GluSnFRs with a broad range of K_d's (i.e., 300 nM, 2.5 μM, 20 μM, and 700 μM) to better suit the detection of physiological glutamate dynamics at the surface of neurons.[63]

As intramolecular FRET reporter responses can be dramatically improved by adjusting their orientation by linker variation,[48,55,64] a linker-truncation library of GluSnFRs was engineered and screened. The best mutant, named SuperGluSnFR, exhibited 44% ΔR_{max}, a 6.2-fold improvement over the original GluSnFR on cell surfaces, with an apparent K_d of 2.5 μM for glutamate. When expressed on the surfaces of dissociated hippocampal neurons, SuperGluSnFR permitted quantitative optical measurements of the time course of synaptic glutamate release, spillover, and reuptake with centisecond temporal and spine-sized spatial resolution.[63]

A SINGLE-FP-BASED GLUTAMATE INDICATOR, iGluSnFR

Though FRET-based glutamate sensors are useful for a number of biological applications as discussed above, their intrinsic properties cannot match the challenging signal-to-noise ratio (SNR) requirements for in vivo imaging of glutamate dynamics in intact brains. In the case of recently optimized calcium and voltage sensors, intensity-based single-FP sensors have superior dynamic ranges, kinetics, SNRs, and photostability when compared to FRET-based sensors.[27,28,33] To improve the performance further and to expand the applications of glutamate sensors in neuroscience, an ultrasensitive, single-FP-based glutamate indicator, iGluSnFR, based on GltI, was developed. In iGluSnFR (Figure 2B), cpGFP is properly positioned in GltI such that glutamate-binding-induced conformational changes result in changes to the chromophore environment, thus transforming ligand-binding events to increased fluorescence. iGluSnFR allows in situ detection of physiological levels of glutamate release and uptake in dissociated neuronal culture, acute brain slices, and behaving mice.[65] Here using iGluSnFR as an example, we review established glutamate sensor design and optimization pipelines that will be needed to move sensors from the realm of concept through purified protein experiments, into cultured cells, brain slices, and, ultimately, in vivo experiments.

The high-resolution crystal structure of glutamate-bound GltI (PDB ID: 2VHA, Figure 3A) from *Shigella flexneri*, which shares 99% homology with *E. coli* GltI, has been solved.[65,66] This structure revealed atomic details of glutamate binding mechanisms, providing a template for systematic computational-based protein engineering efforts.[66] First, to determine the proper insertion site of cpGFP in GltI, Marvin et al. plotted Cα torsion angle differences to identify ligand-dependent structural changes in sequentially adjacent residues, which resulted in three potential cpGFP insertion sites. One insertion point close to the interdomain hinge region yielded the best fluorescent changes ($\Delta F/F$). Second, to improve sensor dynamics and kinetics further, the authors performed a linker optimization with site-saturated mutagenesis and length optimization. Then, to display the sensor on the surface of cells for sensing glutamate release and uptake, cpGFP-fused GltI was inserted into a revised pDisplay vector consisting of an N-terminal immunoglobulin κ-chain leader sequence and a C-terminal transmembrane anchoring domain of platelet-derived growth factor receptor. Finally, systematic characterization and validation of lead variants was performed, including photophysical characterization under both one and two-photon illumination. Glutamate binding specificity and multiple-step validation in HEK 293 cells, dissociated neuronal culture, brain slices, and behaving animals were also carried out for lead variants. The best variant, iGluSnFR, demonstrated sufficient sensitivity ($\Delta F/F_{max}$ = 1.03, K_d = 4.9 μM) and photostability to permit direct in vivo optical measurement of glutamate transients in single dendritic spines, as well as dendritic branches. iGluSnFR is compatible with high-frequency scans (e.g., >2000 Hz line scans, ~100 Hz frame scans) and responds with single millisecond temporal resolution to two-photon glutamate uncaging in acute hippocampal slices.[65]

DIRECT OPTICAL MEASUREMENT OF GLUTAMATE DYNAMICS

Several classes of phenomena currently under study in neuroscience would benefit from the spatial and temporal

DOI: 10.1021/cn500280k
ACS Chem. Neurosci. 2015, 6, 84−93

resolution that genetically encoded NT sensors offer. For example, neural cells have highly complex morphological features (e.g., dendritic spines, axons) that allow compartmentalization of computations performed on incoming information. The spatiotemporal pattern with which synaptic signals impinge upon these subcellular compartments determines the response properties[67−71] and tendency toward plasticity[72,73] of a cell. Such patterns of activation have historically proven difficult to study with both spatial and temporal precision, yet genetically encoded NT sensors are well suited to this need. Indeed, genetically encoded glutamate sensors, such as iGluSnFR, have already been deployed to track synaptic glutamate transients in real time in in situ[65,74−76] and in vivo[65] experimental preparations. These studies have provided details about how stimulus selectivity arises in direction-selective cells in the retina;[76] and how temporal specificity is achieved by OFF bipolar cells (a subgroup of bipolar cells expressing ionotropic glutamate receptors and becoming depolarized in the dark in the retina).[75]

It is now known that glutamate,[77,78] GABA,[79,80] and glycine, and to a larger extent DA,[81,82] norepinephrine,[83,84] serotonin,[85−87] and acetylcholine,[88,89] within the central nervous system escape synaptic clefts at physiologically relevant concentrations or are released from nonsynaptic sites in a process known as volume transmission.[90] In this way, these NTs or neuromodulators exert influence on target cells via receptors located at nonsynaptic sites, including receptors expressed by astrocytes. A critical question is to what extent the primary mode of action of a particular NT is synaptic or extrasynaptic in a given brain region under specific conditions. Further, in those cases in which the principal mode is extrasynaptic, which cells or subcellular compartments are exposed to physiologically relevant extracellular concentrations of NT?

Genetically encoded glutamate sensors can be potentially transformative for our understanding of the dynamics of volume transmission of glutamate. These tools have provided a direct readout for the spatial and temporal extent of synaptic spillover of glutamate under various conditions in several brain regions.[41,65] iGluSnFR has been used to track the dynamics of extrasynaptic glutamate at the surface of astrocytes in brain slices.[74] This work is paving the way for a greater understanding of the function of volume transmission of glutamate in the central nervous system.

THE FUTURE OF NT SENSOR DESIGN

For end users, choosing and implementing the most appropriate NT sensors and imaging system (e.g., sensor expression methods, optimizing sensor expression levels to balance between SNR and potential excitotoxicity, photostability and pH-sensitivity of the sensors, optical instrumentation, image acquisition and processing algorithms, etc.) is paramount. In terms of fluorescent calcium imaging, the strengths and weaknesses of available imaging platforms and intrinsic and extrinsic properties of genetically encoded probes in the context of specific applications have been characterized and reviewed elsewhere.[54,55]

Otherwise, the ability to monitor neural activity in large numbers of neurons has been accelerated over the past two decades by optical methods and molecular tools. Though other NT detection methods as discussed above have been broadly used, fluorescent probes remain highly attractive to neuroscientists to decode the dynamics of neural circuitry due to advances in fluorescence microscopy in terms of spatiotemporal resolution to image individual synapses. Compared to fluorescent probes such as synthetic small organic molecules, synthetic genetically encoded hybrid sensors, and cell-based sensors, genetically encoded fluorescent sensors, are especially preferred due to their specific genetic labeling, minimal invasiveness of probe delivery, and high signal-to-noise ratio.

With advances in the optimization of the sensor engineering pipeline, including protein crystallography, computational protein design, and high throughput automated screening platforms, a suite of genetically encoded sensors for a variety of NTs is now ripe for development. The experience of developing and optimizing genetically encoded calcium, voltage, and glutamate sensors can be directly applied to the development of specific, targetable, and ultrasensitive sensors for a number of different NTs and neuromodulators. Here we discuss a few active areas of NT sensor engineering efforts.

Although any proteins that undergo large conformational changes upon binding of a NT can serve as scaffolds for sensor engineering, bacterial PBPs for a variety of metabolic ligands have already proven to be good starting scaffolds for the systematic design of NT sensors in combination with computational design and directed-evolution. Promising candidates for future sensor design include smaller native GABA binding proteins like PBP Atu2422[91] and Atu4243[92] (Figure 3B) from *Agrobacterium tumefaciens* and PFL_0342[93] from *Pseudomonas fluorescens*. These proteins may provide a direct scaffold for engineering GABA sensors. Advances in computational design have enabled de novo design of ligand binding pockets.[94] Therefore, it may be possible to transform the specificity and affinity of scaffold PBPs via computational redesign of ligand-binding pockets to recognize given NTs. For example, it may be possible to redesign the glutamate binding pocket of GltI to bind GABA based on the structural analysis of the GABA-binding pocket of Atu2422 or human $GABA_B$ receptor.[95] Additional optimization of these binding pockets by computationally mutating neighboring amino acids and using directed-evolution will be necessary to tune binding specificity and selectivity.

In addition, extending the color-spectrum of FPs would greatly increase the potential of NT sensors in terms of multiplexed imaging of synapses.[96] For example, multicolor imaging of diverse cell types or synapses could reveal the spatiotemporal relationships between excitatory and inhibitory signals in shaping neural circuitry. Red-shifted NT sensors would reduce tissue scattering and phototoxicity, and facilitate deep imaging. Finally, color-shifted indicators could seamlessly integrate into calcium imaging and optogenetics experiments. Similar to iGluSnFR, it is anticipated that NT sensors will be encoded by DNA and expressed in specific brain regions of interest in a noninvasive way to allow tracking of NT dynamics and signaling at specific synaptic classes, as well as to interrogate the interactions of neurotransmitters within genetically identified cell populations at both synaptic and extrasynaptic sites.

REAGENT AVAILABILITY

FLIPE and iGluSnFR driven by CMV and T7 promoter are available from Addgene. AAV virus and pAAV constructs for iGluSnFR are available from the University of Pennsylvania Vector Core, driven by a *synapsin-1* or GFAP promoter (http://www.med.upenn.edu/gtp/vectorcore/Catalogue.shtml).

DOI: 10.1021/cn500280k
ACS Chem. Neurosci. 2015, 6, 84−93

AUTHOR INFORMATION

Corresponding Author

*E-mail: lintian@ucdavis.edu.

Funding

This work was supported by an NIH director's New Innovator Award (DP2OD019427), a BRAIN Initiative U01 (U01NS090604, National Institute of Neurological Disorders and Stroke), and a Human Frontier Young Investigator Award.

Notes

The authors declare no competing financial interest.

ACKNOWLEDGMENTS

We would like to thank Dr. Anne Andrews for critical feedback on the manuscript. Molecular graphics and analyses were performed using Chimera developed at University of California, San Francisco (supported by NIGMS P41-GM103311).

REFERENCES

(1) De-Miguel, F. F., and Fuxe, K. (2012) Extrasynaptic neurotransmission as a way of modulating neuronal functions. *Front. Physiol. 3*, 16.

(2) Branco, T., and Staras, K. (2009) The probability of neurotransmitter release: Variability and feedback control at single synapses. *Nat. Rev. Neurosci. 10*, 373−383.

(3) Ziburkus, J., Cressman, J. R., and Schiff, S. J. (2013) Seizures as imbalanced up states: excitatory and inhibitory conductances during seizure-like events. *J. Neurophysiol. 109*, 1296−1306.

(4) van Spronsen, M., and Hoogenraad, C. C. (2010) Synapse pathology in psychiatric and neurologic disease. *Curr. Neurol. Neurosci. Rep. 10*, 207−214.

(5) Hyman, S. E. (2005) Neurotransmitters. *Curr. Biol. 15*, R154−158.

(6) Wightman, R. M. (2006) Detection technologies. Probing cellular chemistry in biological systems with microelectrodes. *Science 311*, 1570−1574.

(7) Kennedy, R. T. (2013) Emerging trends in in vivo neurochemical monitoring by microdialysis. *Curr. Opin. Chem. Biol. 17*, 860−867.

(8) Ferris, M. J., Calipari, E. S., Yorgason, J. T., and Jones, S. R. (2013) Examining the complex regulation and drug-induced plasticity of dopamine release and uptake using voltammetry in brain slices. *ACS Chem. Neurosci. 4*, 693−703.

(9) Keithley, R. B., Takmakov, P., Bucher, E. S., Belle, A. M., Owesson-White, C. A., Park, J., and Wightman, R. M. (2011) Higher sensitivity dopamine measurements with faster-scan cyclic voltammetry. *Anal. Chem. 83*, 3563−3571.

(10) Chefer, V. I., Thompson, A. C., Zapata, A., and Shippenberg, T. S. (2009) Overview of brain microdialysis. *Curr. Protoc. Neurosci.*, DOI: 10.1002/0471142301.ns0701s47.

(11) Hu, Y., Mitchell, K. M., Albahadily, F. N., Michaelis, E. K., and Wilson, G. S. (1994) Direct measurement of glutamate release in the brain using a dual enzyme-based electrochemical sensor. *Brain Res. 659*, 117−125.

(12) Dale, N., Hatz, S., Tian, F., and Llaudet, E. (2005) Listening to the brain: Microelectrode biosensors for neurochemicals. *Trends Biotechnol. 23*, 420−428.

(13) Tuominen, L., Nummenmaa, L., Keltikangas-Jarvinen, L., Raitakari, O., and Hietala, J. (2014) Mapping neurotransmitter networks with PET: An example on serotonin and opioid systems. *Hum. Brain Mapp. 35*, 1875−1884.

(14) Meyer-Lindenberg, A. (2010) From maps to mechanisms through neuroimaging of schizophrenia. *Nature 468*, 194−202.

(15) Lee, T., Cai, L. X., Lelyveld, V. S., Hai, A., and Jasanoff, A. (2014) Molecular-level functional magnetic resonance imaging of dopaminergic signaling. *Science 344*, 533−535.

(16) Shapiro, M. G., Westmeyer, G. G., Romero, P. A., Szablowski, J. O., Kuster, B., Shah, A., Otey, C. R., Langer, R., Arnold, F. H., and Jasanoff, A. (2010) Directed evolution of a magnetic resonance imaging contrast agent for noninvasive imaging of dopamine. *Nat. Biotechnol. 28*, 264−270.

(17) Brustad, E. M., Lelyveld, V. S., Snow, C. D., Crook, N., Jung, S. T., Martinez, F. M., Scholl, T. J., Jasanoff, A., and Arnold, F. H. (2012) Structure-guided directed evolution of highly selective p450-based magnetic resonance imaging sensors for dopamine and serotonin. *J. Mol. Biol. 422*, 245−262.

(18) Kobat, D., Horton, N. G., and Xu, C. (2011) In vivo two-photon microscopy to 1.6-mm depth in mouse cortex. *J. Biomed. Opt. 16*, 106014.

(19) Cheng, L.-C., Horton, N. G., Wang, K., Chen, S.-J., and Xu, C. (2014) Measurements of multiphoton action cross sections for multiphoton microscopy. *Biomed. Opt. Express 5*, 3427−3433.

(20) Ouzounov, D. G., Horton, N., Wang, T., Feng, D., Nishimura, N., and Xu, C. (2014) In Vivo Three-photon Calcium Imaging of Brain Activity from Layer 6 Neurons in Mouse Brain, In *CLEO: 2014 Postdeadline Paper Digest*, p STh5C.2, Optical Society of America, San Jose, CA.

(21) Ghosh, K. K., Burns, L. D., Cocker, E. D., Nimmerjahn, A., Ziv, Y., Gamal, A. E., and Schnitzer, M. J. (2011) Miniaturized integration of a fluorescence microscope. *Nat. Methods 8*, 871−878.

(22) Ziv, Y., Burns, L. D., Cocker, E. D., Hamel, E. O., Ghosh, K. K., Kitch, L. J., El Gamal, A., and Schnitzer, M. J. (2013) Long-term dynamics of CA1 hippocampal place codes. *Nat. Neurosci. 16*, 264−266.

(23) Small, A., and Stahlheber, S. (2014) Fluorophore localization algorithms for super-resolution microscopy. *Nat. Methods 11*, 267−279.

(24) Huang, B., Bates, M., and Zhuang, X. (2009) Super-resolution fluorescence microscopy. *Annu. Rev. Biochem. 78*, 993−1016.

(25) Vladimirov, N., Mu, Y., Kawashima, T., Bennett, D. V., Yang, C. T., Looger, L. L., Keller, P. J., Freeman, J., and Ahrens, M. B. (2014) Light-sheet functional imaging in fictively behaving zebrafish. *Nat. Methods 11*, 883−884.

(26) Chen, B. C., Legant, W. R., Wang, K., Shao, L., Milkie, D. E., Davidson, M. W., Janetopoulos, C., Wu, X. S., Hammer, J. A., 3rd, Liu, Z., English, B. P., Mimori-Kiyosue, Y., Romero, D. P., Ritter, A. T., Lippincott-Schwartz, J., Fritz-Laylin, L., Mullins, R. D., Mitchell, D. M., Bembenek, J. N., Reymann, A. C., Bohme, R., Grill, S. W., Wang, J. T., Seydoux, G., Tulu, U. S., Kiehart, D. P., and Betzig, E. (2014) Lattice light-sheet microscopy: imaging molecules to embryos at high spatiotemporal resolution. *Science 346*, 1257998.

(27) Chen, T. W., Wardill, T. J., Sun, Y., Pulver, S. R., Renninger, S. L., Baohan, A., Schreiter, E. R., Kerr, R. A., Orger, M. B., Jayaraman, V., Looger, L. L., Svoboda, K., and Kim, D. S. (2013) Ultrasensitive fluorescent proteins for imaging neuronal activity. *Nature 499*, 295−300.

(28) Tian, L., Hires, S. A., Mao, T., Huber, D., Chiappe, M. E., Chalasani, S. H., Petreanu, L., Akerboom, J., McKinney, S. A., Schreiter, E. R., Bargmann, C. I., Jayaraman, V., Svoboda, K., and Looger, L. L. (2009) Imaging neural activity in worms, flies and mice with improved GCaMP calcium indicators. *Nat. Methods 6*, 875−881.

(29) Akerboom, J., Chen, T. W., Wardill, T. J., Tian, L., Marvin, J. S., Mutlu, S., Calderon, N. C., Esposti, F., Borghuis, B. G., Sun, X. R., Gordus, A., Orger, M. B., Portugues, R., Engert, F., Macklin, J. J., Filosa, A., Aggarwal, A., Kerr, R. A., Takagi, R., Kracun, S., Shigetomi, E., Khakh, B. S., Baier, H., Lagnado, L., Wang, S. S., Bargmann, C. I., Kimmel, B. E., Jayaraman, V., Svoboda, K., Kim, D. S., Schreiter, E. R., and Looger, L. L. (2012) Optimization of a GCaMP calcium indicator for neural activity imaging. *J. Neurosci. 32*, 13819−13840.

(30) Miesenbock, G., De Angelis, D. A., and Rothman, J. E. (1998) Visualizing secretion and synaptic transmission with pH-sensitive green fluorescent proteins. *Nature 394*, 192−195.

(31) Li, Y., and Tsien, R. W. (2012) pHTomato, a red, genetically encoded indicator that enables multiplex interrogation of synaptic activity. *Nat. Neurosci. 15*, 1047−1053.

DOI: 10.1021/cn500280k
ACS Chem. Neurosci. 2015, 6, 84−93

(32) Zhu, Y., Xu, J., and Heinemann, S. F. (2009) Two pathways of synaptic vesicle retrieval revealed by single-vesicle imaging. *Neuron 61*, 397−411.
(33) St-Pierre, F., Marshall, J. D., Yang, Y., Gong, Y., Schnitzer, M. J., and Lin, M. Z. (2014) High-fidelity optical reporting of neuronal electrical activity with an ultrafast fluorescent voltage sensor. *Nat. Neurosci. 17*, 884−889.
(34) Jin, L., Han, Z., Platisa, J., Wooltorton, J. R., Cohen, L. B., and Pieribone, V. A. (2012) Single action potentials and subthreshold electrical events imaged in neurons with a fluorescent protein voltage probe. *Neuron 75*, 779−785.
(35) Gong, Y., Wagner, M. J., Li, J. Z., and Schnitzer, M. J. (2014) Imaging neural spiking in brain tissue using FRET-opsin protein voltage sensors. *Nat. Commun. 5*, 3674.
(36) Dodge, F. A., Jr., and Rahamimoff, R. (1967) Co-operative action a calcium ions in transmitter release at the neuromuscular junction. *J. Physiol. 193*, 419−432.
(37) Singer, J. H., and Diamond, J. S. (2006) Vesicle depletion and synaptic depression at a mammalian ribbon synapse. *J. Neurophysiol. 95*, 3191−3198.
(38) Gubernator, N. G., Zhang, H., Staal, R. G., Mosharov, E. V., Pereira, D. B., Yue, M., Balsanek, V., Vadola, P. A., Mukherjee, B., Edwards, R. H., Sulzer, D., and Sames, D. (2009) Fluorescent false neurotransmitters visualize dopamine release from individual presynaptic terminals. *Science 324*, 1441−1444.
(39) Rodriguez, P. C., Pereira, D. B., Borgkvist, A., Wong, M. Y., Barnard, C., Sonders, M. S., Zhang, H., Sames, D., and Sulzer, D. (2013) Fluorescent dopamine tracer resolves individual dopaminergic synapses and their activity in the brain. *Proc. Natl. Acad. Sci. U. S. A. 110*, 870−875.
(40) Namiki, S., Sakamoto, H., Iinuma, S., Iino, M., and Hirose, K. (2007) Optical glutamate sensor for spatiotemporal analysis of synaptic transmission. *Eur. J. Neurosci. 25*, 2249−2259.
(41) Okubo, Y., Sekiya, H., Namiki, S., Sakamoto, H., Iinuma, S., Yamasaki, M., Watanabe, M., Hirose, K., and Iino, M. (2010) Imaging extrasynaptic glutamate dynamics in the brain. *Proc. Natl. Acad. Sci. U. S. A. 107*, 6526−6531.
(42) Okubo, Y., and Iino, M. (2011) Visualization of glutamate as a volume transmitter. *J. Physiol. 589*, 481−488.
(43) Brun, M. A., Griss, R., Reymond, L., Tan, K. T., Piguet, J., Peters, R. J., Vogel, H., and Johnsson, K. (2011) Semisynthesis of fluorescent metabolite sensors on cell surfaces. *J. Am. Chem. Soc. 133*, 16235−16242.
(44) Masharina, A., Reymond, L., Maurel, D., Umezawa, K., and Johnsson, K. (2012) A fluorescent sensor for GABA and synthetic GABA(B) receptor ligands. *J. Am. Chem. Soc. 134*, 19026−19034.
(45) Brun, M. A., Tan, K. T., Griss, R., Kielkowska, A., Reymond, L., and Johnsson, K. (2012) A semisynthetic fluorescent sensor protein for glutamate. *J. Am. Chem. Soc. 134*, 7676−7678.
(46) Nguyen, Q. T., Schroeder, L. F., Mank, M., Muller, A., Taylor, P., Griesbeck, O., and Kleinfeld, D. (2010) An in vivo biosensor for neurotransmitter release and in situ receptor activity. *Nat. Neurosci. 13*, 127−132.
(47) Muller, A., Joseph, V., Slesinger, P. A., and Kleinfeld, D. (2014) Cell-based reporters reveal in vivo dynamics of dopamine and norepinephrine release in murine cortex. *Nat. Methods 11*, 1245−1252.
(48) Baird, G. S., Zacharias, D. A., and Tsien, R. Y. (1999) Circular permutation and receptor insertion within green fluorescent proteins. *Proc. Natl. Acad. Sci. U. S. A. 96*, 11241−11246.
(49) Wang, Q., Shui, B., Kotlikoff, M. I., and Sondermann, H. (2008) Structural basis for calcium sensing by GCaMP2. *Structure 16*, 1817−1827.
(50) Akerboom, J., Rivera, J. D., Guilbe, M. M., Malave, E. C., Hernandez, H. H., Tian, L., Hires, S. A., Marvin, J. S., Looger, L. L., and Schreiter, E. R. (2009) Crystal structures of the GCaMP calcium sensor reveal the mechanism of fluorescence signal change and aid rational design. *J. Biol. Chem. 284*, 6455−6464.
(51) Nagai, T., Sawano, A., Park, E. S., and Miyawaki, A. (2001) Circularly permuted green fluorescent proteins engineered to sense Ca^{2+}. *Proc. Natl. Acad. Sci. U. S. A. 98*, 3197−3202.
(52) Miyawaki, A., Llopis, J., Heim, R., McCaffery, J. M., Adams, J. A., Ikura, M., and Tsien, R. Y. (1997) Fluorescent indicators for Ca^{2+} based on green fluorescent proteins and calmodulin. *Nature 388*, 882−887.
(53) Lindenburg, L., and Merkx, M. (2014) Engineering genetically encoded FRET sensors. *Sensors 14*, 11691−11713.
(54) Tian, L., Akerboom, J., Schreiter, E. R., and Looger, L. L. (2012) Neural activity imaging with genetically encoded calcium indicators. *Prog. Brain Res. 196*, 79−94.
(55) Broussard, G. J., Liang, R., and Tian, L. (2014) Monitoring activity in neural circuits with genetically encoded indicators. *Front. Mol. Neurosci. 7*, 97.
(56) Dwyer, M. A., and Hellinga, H. W. (2004) Periplasmic binding proteins: A versatile superfamily for protein engineering. *Curr. Opin. Struct. Biol. 14*, 495−504.
(57) Berntsson, R. P., Smits, S. H., Schmitt, L., Slotboom, D. J., and Poolman, B. (2010) A structural classification of substrate-binding proteins. *FEBS Lett. 584*, 2606−2617.
(58) de Lorimier, R. M., Smith, J. J., Dwyer, M. A., Looger, L. L., Sali, K. M., Paavola, C. D., Rizk, S. S., Sadigov, S., Conrad, D. W., Loew, L., and Hellinga, H. W. (2002) Construction of a fluorescent biosensor family. *Protein Sci. 11*, 2655−2675.
(59) Okumoto, S., Looger, L. L., Micheva, K. D., Reimer, R. J., Smith, S. J., and Frommer, W. B. (2005) Detection of glutamate release from neurons by genetically encoded surface-displayed FRET nanosensors. *Proc. Natl. Acad. Sci. U. S. A. 102*, 8740−8745.
(60) Dulla, C., Tani, H., Okumoto, S., Frommer, W. B., Reimer, R. J., and Huguenard, J. R. (2008) Imaging of glutamate in brain slices using FRET sensors. *J. Neurosci. Methods 168*, 306−319.
(61) Deuschle, K., Okumoto, S., Fehr, M., Looger, L. L., Kozhukh, L., and Frommer, W. B. (2005) Construction and optimization of a family of genetically encoded metabolite sensors by semirational protein engineering. *Protein Sci. 14*, 2304−2314.
(62) Tsien, R. Y. (2005) Building and breeding molecules to spy on cells and tumors. *FEBS Lett. 579*, 927−932.
(63) Hires, S. A., Zhu, Y., and Tsien, R. Y. (2008) Optical measurement of synaptic glutamate spillover and reuptake by linker optimized glutamate-sensitive fluorescent reporters. *Proc. Natl. Acad. Sci. U. S. A. 105*, 4411−4416.
(64) Nagai, T., Yamada, S., Tominaga, T., Ichikawa, M., and Miyawaki, A. (2004) Expanded dynamic range of fluorescent indicators for Ca^{2+} by circularly permuted yellow fluorescent proteins. *Proc. Natl. Acad. Sci. U. S. A. 101*, 10554−10559.
(65) Marvin, J. S., Borghuis, B. G., Tian, L., Cichon, J., Harnett, M. T., Akerboom, J., Gordus, A., Renninger, S. L., Chen, T. W., Bargmann, C. I., Orger, M. B., Schreiter, E. R., Demb, J. B., Gan, W. B., Hires, S. A., and Looger, L. L. (2013) An optimized fluorescent probe for visualizing glutamate neurotransmission. *Nat. Methods 10*, 162−170.
(66) Hu, Y., Fan, C. P., Fu, G., Zhu, D., Jin, Q., and Wang, D. C. (2008) Crystal structure of a glutamate/aspartate binding protein complexed with a glutamate molecule: structural basis of ligand specificity at atomic resolution. *J. Mol. Biol. 382*, 99−111.
(67) Jeffress, L. A. (1948) A place theory of sound localization. *J. Comp. Physiol. Psychol. 41*, 35−39.
(68) Joris, P. X., Smith, P. H., and Yin, T. C. (1998) Coincidence detection in the auditory system: 50 years after Jeffress. *Neuron 21*, 1235−1238.
(69) Hubel, D. H., and Wiesel, T. N. (1962) Receptive fields, binocular interaction and functional architecture in the cat's visual cortex. *J. Physiol. 160*, 106−154.
(70) Chapman, B., Zahs, K. R., and Stryker, M. P. (1991) Relation of cortical cell orientation selectivity to alignment of receptive fields of the geniculocortical afferents that arborize within a single orientation column in ferret visual cortex. *J. Neurosci. 11*, 1347−1358.

DOI: 10.1021/cn500280k
ACS Chem. Neurosci. 2015, 6, 84−93

(71) Reid, R. C., and Alonso, J. M. (1995) Specificity of monosynaptic connections from thalamus to visual cortex. *Nature 378*, 281−284.
(72) Hebb, D. O. (1949) *The Organization of Behavior: A Neuropsychological Theory*, John Wiley And Sons, Inc., New York.
(73) Bliss, T. V., and Lomo, T. (1973) Long-lasting potentiation of synaptic transmission in the dentate area of the anaesthetized rabbit following stimulation of the perforant path. *J. Physiol. 232*, 331−356.
(74) Haustein, M. D., Kracun, S., Lu, X. H., Shih, T., Jackson-Weaver, O., Tong, X., Xu, J., Yang, X. W., O'Dell, T. J., Marvin, J. S., Ellisman, M. H., Bushong, E. A., Looger, L. L., and Khakh, B. S. (2014) Conditions and constraints for astrocyte calcium signaling in the hippocampal mossy fiber pathway. *Neuron 82*, 413−429.
(75) Borghuis, B. G., Looger, L. L., Tomita, S., and Demb, J. B. (2014) Kainate receptors mediate signaling in both transient and sustained OFF bipolar cell pathways in mouse retina. *J. Neurosci. 34*, 6128−6139.
(76) Park, S. J., Kim, I. J., Looger, L. L., Demb, J. B., and Borghuis, B. G. (2014) Excitatory synaptic inputs to mouse on-off direction-selective retinal ganglion cells lack direction tuning. *J. Neurosci. 34*, 3976−3981.
(77) Kullmann, D. M., Erdemli, G., and Asztely, F. (1996) LTP of AMPA and NMDA receptor-mediated signals: evidence for presynaptic expression and extrasynaptic glutamate spill-over. *Neuron 17*, 461−474.
(78) Rusakov, D. A., and Kullmann, D. M. (1998) Extrasynaptic glutamate diffusion in the hippocampus: ultrastructural constraints, uptake, and receptor activation. *J. Neurosci. 18*, 3158−3170.
(79) Scanziani, M. (2000) GABA spillover activates postsynaptic GABA(B) receptors to control rhythmic hippocampal activity. *Neuron 25*, 673−681.
(80) Beenhakker, M. P., and Huguenard, J. R. (2010) Astrocytes as gatekeepers of GABAB receptor function. *J. Neurosci. 30*, 15262−15276.
(81) Cragg, S. J., and Rice, M. E. (2004) DAncing past the DAT at a DA synapse. *Trends Neurosci 27*, 270−277.
(82) Arbuthnott, G. W., and Wickens, J. (2007) Space, time and dopamine. *Trends Neurosci 30*, 62−69.
(83) Aoki, C., Venkatesan, C., Go, C. G., Forman, R., and Kurose, H. (1998) Cellular and subcellular sites for noradrenergic action in the monkey dorsolateral prefrontal cortex as revealed by the immunocytochemical localization of noradrenergic receptors and axons. *Cereb. Cortex 8*, 269−277.
(84) Bekar, L. K., He, W., and Nedergaard, M. (2008) Locus coeruleus alpha-adrenergic-mediated activation of cortical astrocytes in vivo. *Cereb. Cortex 18*, 2789−2795.
(85) Bunin, M. A., and Wightman, R. M. (1998) Quantitative evaluation of 5-hydroxytryptamine (serotonin) neuronal release and uptake: an investigation of extrasynaptic transmission. *J. Neurosci. 18*, 4854−4860.
(86) Bunin, M. A., and Wightman, R. M. (1999) Paracrine neurotransmission in the CNS: Involvement of 5-HT. *Trends Neurosci 22*, 377−382.
(87) De-Miguel, F. F., and Trueta, C. (2005) Synaptic and extrasynaptic secretion of serotonin. *Cell. Mol. Neurobiol. 25*, 297−312.
(88) Descarries, L., and Mechawar, N. (2000) Ultrastructural evidence for diffuse transmission by monoamine and acetylcholine neurons of the central nervous system. *Prog. Brain Res. 125*, 27−47.
(89) Navarrete, M., Perea, G., Fernandez de Sevilla, D., Gomez-Gonzalo, M., Nunez, A., Martin, E. D., and Araque, A. (2012) Astrocytes mediate in vivo cholinergic-induced synaptic plasticity. *PLoS Biol. 10*, e1001259.
(90) Agnati, L. F., Fuxe, K., Zoli, M., Ozini, I., Toffano, G., and Ferraguti, F. (1986) A correlation analysis of the regional distribution of central enkephalin and beta-endorphin immunoreactive terminals and of opiate receptors in adult and old male rats. Evidence for the existence of two main types of communication in the central nervous system: the volume transmission and the wiring transmission. *Acta Physiol. Scand. 128*, 201−207.
(91) Planamente, S., Vigouroux, A., Mondy, S., Nicaise, M., Faure, D., and Morera, S. (2010) A conserved mechanism of GABA binding and antagonism is revealed by structure-function analysis of the periplasmic binding protein Atu2422 in Agrobacterium tumefaciens. *J. Biol. Chem. 285*, 30294−30303.
(92) Planamente, S., Mondy, S., Hommais, F., Vigouroux, A., Morera, S., and Faure, D. (2012) Structural basis for selective GABA binding in bacterial pathogens. *Mol. Microbiol. 86*, 1085−1099.
(93) Paulsen, I. T., Press, C. M., Ravel, J., Kobayashi, D. Y., Myers, G. S., Mavrodi, D. V., DeBoy, R. T., Seshadri, R., Ren, Q., Madupu, R., Dodson, R. J., Durkin, A. S., Brinkac, L. M., Daugherty, S. C., Sullivan, S. A., Rosovitz, M. J., Gwinn, M. L., Zhou, L., Schneider, D. J., Cartinhour, S. W., Nelson, W. C., Weidman, J., Watkins, K., Tran, K., Khouri, H., Pierson, E. A., Pierson, L. S., 3rd, Thomashow, L. S., and Loper, J. E. (2005) Complete genome sequence of the plant commensal Pseudomonas fluorescens Pf-5. *Nat. Biotechnol. 23*, 873−878.
(94) Tinberg, C. E., Khare, S. D., Dou, J., Doyle, L., Nelson, J. W., Schena, A., Jankowski, W., Kalodimos, C. G., Johnsson, K., Stoddard, B. L., and Baker, D. (2013) Computational design of ligand-binding proteins with high affinity and selectivity. *Nature 501*, 212−216.
(95) Geng, Y., Bush, M., Mosyak, L., Wang, F., and Fan, Q. R. (2013) Structural mechanism of ligand activation in human GABA(B) receptor. *Nature 504*, 254−259.
(96) Akerboom, J., Carreras Calderon, N., Tian, L., Wabnig, S., Prigge, M., Tolo, J., Gordus, A., Orger, M. B., Severi, K. E., Macklin, J. J., Patel, R., Pulver, S. R., Wardill, T. J., Fischer, E., Schuler, C., Chen, T. W., Sarkisyan, K. S., Marvin, J. S., Bargmann, C. I., Kim, D. S., Kugler, S., Lagnado, L., Hegemann, P., Gottschalk, A., Schreiter, E. R., and Looger, L. L. (2013) Genetically encoded calcium indicators for multi-color neural activity imaging and combination with optogenetics. *Front. Mol. Neurosci. 6*, 2.

DOI: 10.1021/cn500280k
ACS Chem. Neurosci. 2015, 6, 84−93